Accepted Article

DR GANG BAI (Orcid ID : 0000-0001-9161-2173)

Received Date : 07-May-2019

Revised Date : 10-Sep-2019

Accepted Date : 29-Oct-2019

Research Article

A natural AKT inhibitor swertiamarin targets AKT-PH domain, inhibits downstream signaling and alleviates inflammation

Running Title: Swertiamarin alleviates inflammation by targeting AKT-PH domain

Man Zhang[a], Xiaoyao Ma[a], Honglei Xu[a], Wenbo Wu[a], XinHe[a], Xiaoying Wang[b], Min Jiang[a], Yuanyuan Hou[a*], Gang Bai[a*]

[a] State Key Laboratory of Medicinal Chemical Biology, College of Pharmacy and Tianjin Key Laboratory of Molecular Drug Research, Nankai University, Haihe Education Park, 38 Tongyan Road, Tianjin, 300353, People's Republic of China; 18202572363@163.com (M.Z.); mxy83396376@163.com (X.M.);

This article has been accepted for publication and undergone full peer review but has not been through the copyediting, typesetting, pagination and proofreading process, which may lead to differences between this version and the Version of Record. Please cite this article as doi: 10.1111/FEBS.15112

This article is protected by copyright. All rights reserved

xuhonglei1994@163.com (H.X.); 2120171287@mail.nankai.edu.cn (W.W.); xinhe@mail.nankai.edu.cn (X. H.); minjiang@nankai.edu.cn (M.J.); houyy@nankai.edu.cn (Y.H.); gangbai@nankai.edu.cn (G.B.)

[b] Tianjin University of Traditional Chinese Medicine, Tianjin, 300193, People's Republic of China; wxy@tjutcm.edu.cn (XY.W.)

* Corresponding author: Yuanyuan Hou, Gang Bai

Tel / Fax: +86-022-23506792 (Yuanyuan Hou, Gang Bai)

E-mail address: houyy@nankai.edu.cn (Yuanyuan Hou), gangbai@nankai.edu.cn (Gang Bai)

Keywords: swertiamarin; anti-inflammation; AKT; PH domain; inhibitor

Abbreviations: SW, Swertiamarin; FLJ, *Flos Lonicerae Japonicae*; Dex, Dexamethasone; LPS, lipopolysaccharide; PA 14, *Pseudomonas aeruginosa* strain PA 14; absMMs, alkyne modified biotin-streptavidin magnetic microspheres.

Abstract

Swertiamarin (SW), a representative component in *Flos Lonicerae Japonicae*, has been reported to exert significant activity in preventing infections. In this research, we aim to clarify the details of SW and its target to explore SW's underlying anti-inflammatory mechanisms. An azide labeled SW probe was synthesized for protein target fishing, and the results demonstrated that AKT could be captured specifically. Immunofluorescence co-localization with AKT was implemented by a click reaction of the SW probe and alkynyl CY5. The result showed that AKT was one of the targets of SW. Then, a competitive combination experiment using a set of AKT inhibitors and a membrane translocation experiment confirmed that SW might target the pleckstrin homology (PH) domain of AKT. This specific binding directly deactivated the phosphorylation of AKT on both Ser473 and Thr308, which induced the dephosphorylation of IKK and NF-κB. Finally, proinflammatory cytokines (TNF-α, IL-6 and IL-8) were suppressed both in cells and acute lung injury animal model by targeting AKT-PH domain. This study demonstrated that SW functions as a natural AKT inhibitor and presents significant anti-inflammatory activity by directly regulating the AKT-PH domain and inhibiting downstream inflammatory molecules.

This article is protected by copyright. All rights reserved

Accepted Article

Accepted Article

Introduction

Inflammation is a complex disease response, which can arise in any tissue in response to traumatic events, post-ischemia, and infectious or toxic agents [1]. Occasionally, it is a protective response to injury and microbial invasion, restoring tissue or organs for recovery [2]. In most cases, inflammation can diminish the beneficial effects of therapy [3]. Inflammation is also considered to be a characteristic of many human diseases, such as diabetes, cardiovascular disorders, cancers, and arthritis [4]. Most of the important signaling pathways, including the TLR4/MYD88 pathway, PI3K-AKT pathway, MAPK pathway, NF-κB pathway and the TNF pathway are all related to inflammation regulation [5-8].

Previous research has demonstrated that a lot of small molecules showed significant activity in anti-inflammatory. Different from antibiotics and nonsteroidal anti-inflammatory drugs, herbal medicine has unique anti-inflammatory mechanism [9]. For example, 8-prenyl quercetin, a respective prenylflavonoid compound, shows the anti-inflammatory effect that was proved to target SEK1-JNK1/2 and MEK1-EARK1/2 in both cell and animal models [10]. Ursolic acid targets to caspase3 and alleviates the downstream factors in anti-inflammation [11]. The explicit mechanism of these molecules provided a better understanding of how these nutrients worked and made them as new potential drugs in regulation physical function.

Lonicera japonica Thunb. (Caprifoliaceae) is one of the oldest Chinese medicine herbs, which is also a common drink in our daily life [12, 13]. *Flos Lonicerae Japonicae* (FLJ) are the flower buds of *Lonicera japonica* possessing wide pharmacological effects, such as anti-inflammatory, antibacterial, antiviral, antiendotoxin, antipyretic and other activities [14, 15]. People likely to drink FLJ tea, which is a kind of healthy beverage for preventing inflammatory diseases, especially in Asia. Several bioactive compounds, including chlorogenic acid, SW and sweroside in FLJ exhibit significant activity for preventing infections. Among the active compounds in FLJ tea, SW, a representative secoiridoid glycoside, exhibits anti-inflammatory, anti-atherosclerotic, antidiabetic and antioxidant activities [16]. Although previous

This article is protected by copyright. All rights reserved

studies have demonstrated that SW provides prominent activity *in vivo* and *in vitro*, while the direct target of SW remains uncharacterized [17].

In the present study, chemical biological approaches were used to prepare different molecular probes of SW for fishing, capturing, imaging and further verifying the target of SW. Subsequently, molecule docking, competitive test and membrane translocation experiment were applied to clarify the binding manner of SW and its target. This research was designed to explain the immune regulation mechanism of SW in details.

Results

SW targets to AKT

To identify the target proteins of SW, a chemical probe of azide labeled SW (probe 1) was synthesized as shown in Fig 1A. The detailed synthesis methods and data of probe 1 were described in the supporting information (Fig S1-S2). Compared with SW, probe 1 showed the similar inhibitory activity of NF-κB, which was detected by dual-bioactive luciferase reporter assay systems (Fig 1B) [19]. The relative luciferase activity for NF-κB was measured according to the Dual-Luciferase Reporter Gene Assay Kit manufacturer's protocol (Promega, WI, USA). Hence, probe 1 was used for fishing the anti-inflammatory targets of SW. As shown in Fig 1C left, enriched proteins were separated by SDS-PAGE and detected with Coomassie Brilliant Blue staining. Compared with the control (Con) group (lane 2), which was treated with the only alkyne modified biotin-streptavidin magnetic microspheres (absMMs), there were few proteins were captured, and much more proteins were captured by probe 1 obviously as shown in lane 3.

To analyze the captured protein targets of SW, PharmMapper was used to predict the potential targets, and the top 30 target proteins were selected for String assay. And the main candidate inflammation-related targets are distributed in three primary pathways, including PI3K-AKT, MAPK and TNF signaling pathways, which were shown in Fig 1D. Among these predicted target proteins, AKT participated in all pathways mentioned above and was recommended as the key target protein of SW. To further verify the prediction, western blot was employed to analyze the enriched proteins. Compared with the Con group

This article is protected by copyright. All rights reserved

(lane 2), the AKT protein band in lane 3 was significantly enriched (Fig 1C right). It suggested that AKT was the primary target protein of SW.

To confirm the interaction between SW and AKT, co-localization of AKT and the CY5 fluorescent tag derivative of probe 1, named SW-CY5, was investigated (Fig 2A). The molecular imaging indicated that the red fluorescence of SW-CY5 in the cytoplasm was observed as shown in Fig 2B. In the Con group, the SW group exhibited minimal fluorescence. The distribution of AKT (green) was detected by incubating AKT antibody and fluorescent secondary antibody. The merge result showed that probe SW-CY5 partially co-localizes with AKT near the membrane of BEAS-2B cells (Yellow), and proved the prediction that SW targets AKT.

SW targets to the PH domain of AKT

To identify the binding pocket of AKT that SW targets, we designed a competition experiment using three types of AKT binding pocket inhibitors. The representative AKT inhibitors include AKT allosteric inhibitor, ATP competitive inhibitor and AKT-PH domain inhibitor [20]. AKT inhibitor VIII, an AKT allosteric inhibitor, blocks AKT in the inactive PH-in conformation via associating with the PH domain residue Trp80 and preventing Thr308 phosphorylation [21]. The ATP competitive inhibitor AT7867 inhibits AKT activity by binding to the ATP site of AKT [22]. And PHT-427 is an AKT-PH domain inhibitor, which inhibits the phosphorylation of AKT as well as its downstream proteins [23]. The experimental procedure was presented in Fig 3A. Firstly, an amino bridging agent coupled with probe 1 was synthesized to attach to the maleic anhydride plates as a solidified probe (probe 2). The detailed information was described in the supporting information (Fig S3-S6). Probe 2 was used to capture free AKT proteins. Then, different types of AKT inhibitors were added to the plates competed with crude AKT proteins or purified AKT-PH domain proteins. The details of expression and purification of AKT-PH domain proteins were described in the supporting information (Fig S7). From the results shown in Fig 3B, only PHT-427, the AKT-PH domain inhibitor and SW can specific competitive the bind of AKT full proteins or AKT-PH domain proteins, and decrease the quantity of AKT or AKT-PH domain that captured by probe 2. The results indicated that SW might similarly target the AKT-PH domain to PHT-427.

This article is protected by copyright. All rights reserved

To further identify the effect of SW on the AKT-PH domain, membrane translocation of the AKT-PH domain affected by SW was detected. The AKT-PH domain fused with a green fluorescent protein (GFP) was used as a marker to observe the membrane transportation of the PH domain in the R25 group. The fluorescence ratios ($AKT^{PH(R25)}$-GFP/Dil) on the cell membrane was used to evaluate the effect of AKT displacement from membranes. As shown in Fig 4A, compared with the specific membrane staining with Dil, the AKT-PH domain activator SC79 demonstrated the effect for preventing AKT-PH domain transfer to the membrane. And the plasma transport of AKT-PH domain was also blocked by SW in a concentration-dependent manner. The above results indicated that SW might act on AKT by targeting to the AKT-PH domain. This specific binding hampers membrane translocation of AKT and affects AKT activity (Fig 4B).

SW inhibits AKT activity and down-regulates AKT phosphorylation levels

To verify the effect of SW acting on the AKT-PH domain, the AKT activation was measured using an AKT kinase kit (Arlington, Ma, USA) according to the manufacturer's instruction. As shown in Fig 5A, SC79 increased AKT activity by directly activate AKT on AKT-PH domain. On the contrary, SW inhibited the activation in a concentration-dependent manner. Besides, western blot was used to investigate the activated forms of AKT. And as shown in Fig 5B, SW reduced the basic level of P-AKT in a concentration-dependent manner the same as PHT-427. SC79 effectively increased the phosphorylation of AKT on both Ser473 and Thr308 (Fig 5C), while the $P\text{-}AKT^{308}$ and $P\text{-}AKT^{473}$ levels were significant decreased with treatment of SW in a dose-dependent manner. The results suggested that SW could not only reduce the basic level of P-AKT, and also abrogate the activation of AKT induced by AKT activator.

Molecular docking of SW and the AKT-PH domain

To specify the interaction between SW and the AKT-PH domain, molecular docking studies were performed to provide further possible binding positions of SW in the AKT-PH domain binding site of AKT (PDB:1UNQ) using MOE software. To determine the best docking model with the lowest energy level, the target protein was docked with the ligands. The binding energy of SW, PHT-427, and SC79 were shown as -5.0668 kcal/mol, -7.3417 kcal/mol and -5.2175 kcal/mol, respectively. As shown in Fig 5C, PHT-427

This article is protected by copyright. All rights reserved

interacts with Asn54, Lys30 and Thr34 residues through hydrogen bonds. Hydrogen bonds with SW were established between the residues Glu49, Lys30, Thr34, and Asp32, which was partly similar to PHT-427. According to the report, Lys30 and Thr34 of the AKT-PH domain are considered critical amino residues, which are intimately associated with AKT inhibition [24]. On the contrary, the activator SC79 was linked with the Lys14, Arg25, and Arg86 residues, yielding a different conformation compared with SW and PHT-427. The molecular docking results explained the possible mechanism of AKT inhibition by SW, which might involve the presentation of a suitable interaction position in the AKT-PH domain.

SW inhibits the signal transduction of downstream inflammatory molecules

To future investigate the effect of SW, RAW264.7 and BEAS-2B cells were used to evaluate AKT phosphorylation respectively. LPS stimulated the Toll-like receptors (TLR), which activated the PI3K-AKT signaling pathway and increased the phosphorylation of AKT in RAW264.7 cells [25]. TNF-α, commonly released by macrophages, can also activate AKT phosphorylation in BEAS-2B cells [26]. PHT-427 was selected as a positive control to contrast with SW. As shown in Fig 6A and 6B, the phosphorylation of AKT on both Ser473 and Thr308 were activated in RAW264.7 cells and BEAS-2B cells, which were induced by LPS and TNF-α, respectively. While the pretreatment with SW and PHT-427 can prevent the activation of AKT significantly. The result suggested that SW acted as an AKT-PH domain inhibitor deactivates AKT phosphorylation, contributes to be a potential anti-inflammation compound.

To detect the effects of SW in the downstream of AKT, the phosphorylation of AKT, IKKα/β and NF-κB and cytokine expression were also examined in BEAS-2B cells. As shown in Fig 6C, AKT, IKKα/β and NF-κB phosphorylation were increased in the LPS-induced group and were markedly suppressed by SW in a dose-response manner. Besides, the groups pretreated with SW significantly suppressed the production of TNF-α, IL-6, and IL-8 induced by LPS (Fig 6D). SW was proved that it no longer acts anti-inflammatory on an AKT-null background (Fig S8). All the results suggested that SW alleviated inflammation via targeting AKT-PH domain and impacted downstream inflammatory molecules.

SW relieves inflammation and suppresses acute lung injury in mice

To verify the anti-inflammatory activity of SW *in vivo*, PA 14 bacteria-induced acute lung injury mice were generated. Firstly, western blot was used to analyze the effects of SW on the activation of AKT and its

This article is protected by copyright. All rights reserved

Accepted Article

downstream proteins. As shown in Fig 7A, compared with the Con group, PA 14 could significantly enhance the level of AKT, IKK and NF-κB phosphorylation. Pretreatment with SW markedly suppressed the phosphorylation of these proteins in lung tissue. In the histological analysis, the lung section in the model (Mod) group presented severe bleeding, widened alveolar septa and cell infiltration compared with the Con group. And SW pretreatment could protect the lung from obvious damage (Fig 7B). In addition, mice pretreated with SW could also decrease the production of TNF-α, IL-6, and IL-8 in lung perfusion (Fig 7C, D, and E). Taken together, the results suggested that SW might inhibit AKT activation and its downstream cytokine storm to relieve acute lung injury.

Discussion

Many iridoid glycosides from natural products have been shown significant anti-inflammatory efficacy [27, 28]. While the targets of these anti-inflammatory ingredients are still unclear. Among the iridoid glycosides, SW as a representative active compound can be detected *in vivo* [29]. Previous studies have demonstrated that SW has been used for treating serum hepatitis [30]. SW also suppressed the release of free radicals induced by phytohemagglutinin neutrophils and regulated expression of proinflammatory cytokine mRNA in LPS-induced macrophages [31]. Furthermore, in Freund's Complete Adjuvant-induced arthritic (AA) rats, SW decreased the levels of p38 MAPK, and markedly modulated proinflammation mediators, caspase 3 and RANKL at both the protein and mRNA levels [32]. In another AA rats model, SW inhibited the development of arthritis by regulating JAK2/STAT3 and NF-κB/IκB signaling pathway, inhibited the expression of proinflammatory cytokines and proangiogenic enzymes, and increased the levels of anti-inflammatory cytokines significantly [33]. In our research, the anti-inflammatory effects and molecular mechanisms of SW were investigated in both animal and cell models. And consistent with the results of previous research, SW showed significant activity in anti-inflammation. Furthermore, SW targeting the AKT-PH domain reduces the phosphorylation of AKT, and influences downstream signaling, cell apoptosis and cell cycle (Fig S9-S10). The result demonstrated the potential of SW for prevention and protection the inflammatory-associated diseases.

Many kinases have become new targets for relief inflammatory and provided the new frontier of anti-inflammation drug development [34]. At the same time, given the critical roles of AKT in many

This article is protected by copyright. All rights reserved

Accepted Article

diseases and pathways, small molecules that target AKT kinases are attractive research objects [35]. AKT/PKB, a serine/threonine protein kinase, plays a central role in both physiological and pathological signaling mechanisms [36]. Three AKT isoforms exist, including PKBα/AKT1, PKBβ/AKT2, and PKBγ/AKT3, which all include an N-terminal pleckstrin homology (PH) domain, a catalytic (kinase) domain, and a C-terminal regulatory part containing a hydrophobic motif (HM) [37]. Small-molecule chemical probes have been widely used to explore fundamental biological mechanisms and processes causing disease, achieving great promise for target explosion [38]. In this study, we applied different chemical biological methods in target fishing, co-localization and competitive inhibitor experiments. From which we finally found that AKT is one of the targets of SW.

In our study, SW was predicted to be a PH-domain inhibitor of AKT, similar to PHT-427. Upon AKT activation, AKT is transferred to the plasma membrane through binding its PH domain with the lipid products of PtdIns (3,4,5) P3 [39]. The interaction of PtdIns (3,4,5) P3 with the AKT-PH domain could not only bring AKT to the membrane but also change the conformation of AKT, exposing two residues, Ser473 and Thr308, for phosphorylation as shown in Fig 4B. Interestingly, AKT-PH domain membrane translocation is not necessary for AKT activation. For example, SC79 prohibits AKT-PH domain translocation to the membrane, but it is an AKT-PH domain activator [36]. In some cases, AKT will become dephosphorylated and inactivated if the binding between AKT-PH domain and PtdIns (3,4,5) P3 was changed. TCN-P, an AKT-PH domain inhibitor, binds to the PH domain of AKT and blocks its recruitment to the plasma membrane to maintain AKT in an inactive conformation, which suggests that this compound may be a potential drug for the treatment of tumors [40, 41]. In our research, we found that SW can inhibit AKT activity dramatically by binding to the PH domain of AKT and block AKT recruitment to the membrane, which can significantly inhibit AKT phosphorylation at Thr308 and Ser473 induced by SC79. Lys14, Arg25, and Arg86 are regarded as key activation sites in the AKT-PH domain [42]. In our research, the AKT-PH domain activator SC79 binds to these three residues. On the contrary, Lys30 and especially Thr34 are considered to be critical amino residues for AKT-PH domain inhibition [24, 43]. Compared with SC79, SW was predicted to bind to the AKT-PH domain at the key residues of Lys30 and Thr34, which is similar to PHT-427. These results explained the reason why only PHT-427 can integrate

This article is protected by copyright. All rights reserved

with AKT that was captured by probe 2 in the competitive experiment.

In our research, SW acted as a natural inhibitor of the AKT-PH domain and presented significant anti-inflammatory efficacy. These results provide an increased understanding of SW, particularly regarding the molecular mechanism of anti-inflammation as well as demonstrating the potential of SW as a therapeutic for the treatment of inflammatory-associated diseases.

Materials and methods

Reagents and materials

SW (purity > 98%, determined by HPLC) was purchased from JingZhu Bio-Tech Co., Ltd. (Nanjing, China). CY5-YNE (alkynyl CY5), AKT-PH domain agonist SC79 and AKT allosteric inhibitor VIII were purchased from MedChemExpress (NJ, USA). AKT-PH domain inhibitor PHT-427 and ATP competitive inhibitor AT7867 were purchased from Selleckchem (Texas, USA). Human TNF-α was purchased from PeproTech (NJ, USA). Alkyne modified biotin was synthesized by Wuxi App Tec (Beijing, China). Streptavidin magnetic microspheres, Tris-triazoleamine, $CuSO_4$, and ascorbate were obtained from Aladdin (Beijing, China). Dexamethasone (Dex) and lipopolysaccharide (LPS) were purchased from Sigma Corporation (MO, USA). Plasmids, including pcDNA3 $AKT^{PH(R25)}$-GFP and $AKT^{PH(R25C)}$-GFP, were purchased from Addgene (MA, USA). 1,1'-dioctadecyl-3,3,3',3'-tetramethylindocarbocyanine (Dil) was purchased from Solarbio (Beijing, China). Primary antibodies against AKT, IKKα/β, NF-κB (p65), β-actin, P-AKT (Thr308 and Ser473), P-IKKα/β, and P- NF-κB (p65) and secondary antibodies were purchased from Cell Signaling Technology (MA, USA). Alexa Fluor 488-conjugated anti-rabbit antibody was purchased from Abcam (MA, UK). AKT activity assay kit was purchased from GenMed Scientific Inc. (MA, USA). Maleic anhydride 96-well plates were purchased from Thermo (Ll, USA). *Pseudomonas aeruginosa* strain PA 14 (PA 14) was obtained from Associate professor Bai Fang group of Nankai University (Tianjin, China). All cell culture reagents were purchased from Gibco BRL Life Technologies (NY, USA).

Cell culture

BEAS-2B cells, RAW264.7 cells and HEK 293T cells were purchased from American Type Culture

This article is protected by copyright. All rights reserved

Collection (Rockville, MD). BEAS-2B cells and RAW264.7 cells were cultured in standard growth media (RPMI Medium 1640, 4.5 g/L glucose, L-glutamine, sodium pyruvate, 10% FBS, 1% penicillin/streptomycin). HEK 293T cells were cultured in standard growth media (DMEM, 4.5 g/L glucose, L-glutamine, sodium pyruvate, 10% FBS, 1% penicillin/streptomycin). All the cells were cultured at 37°C in 5% CO_2 and a humidified incubator.

Target prediction and capturing

The three-dimensional structure of SW with sdf format was imported into PharmMapper data (http://lilab.ecust.edu.cn/pharmmapper/) for reverse molecular docking. According to the result of the scoring function, the top 30 corresponding targets were selected and validated using Protein Interaction Soft String 10.1 (http://string-db.org/) and KEGG (https://www.genome.jp/kegg/pathway.html) network.

For capturing the target protein of SW, the alkyne modified biotin-streptavidin magnetic microspheres (absMMs) were prepared firstly. An azide-SW probe (probe 1) was then synthesized to connect the absMMs. BEAS-2B cells were added with or without probe 1 for 6 h, and then the lysate of cells was collected and used to combine with absMMs overnight on a shaker at 4°C. Finally, the captured proteins were gathered by boiling the absMMs with 0.1% SDS for 5 min, which can untie the combination of biotin and streptavidin. The captured target proteins were detected by Coomassie Brilliant Blue staining and Western blot via above-recommended target antibodies.

Co-localization of target protein with SW probe

BEAS-2B cells were plated on the small confocal dishes until the cells achieved approximately 60% confluence. 10 μM probe 1 or unmodified SW was added to the cells for 2 h administration respectively. After washing with cold PBS three times, the cells were fixed in 4% pre-cooled paraformaldehyde for 15 min. Then, 10 μM alkynyl CY5 fluorescent tag incubated with catalyst solution (20 μM Tris-triazoleamine, 10 μM $CuSO_4$ and 20 μM sodium ascorbate in pre-cooled PBS) was added to the cells with gentle shaking at room temperature for 1 h. 10% goat serum was then added to the cells at room temperature for 30 min to block unspecific binding sites. After that, cells were incubated with AKT (1:400) antibody at 4°C overnight and secondary antibody (Alexa Fluor 488) for 1 h at room temperature. Cells were washed with PBST, and a confocal microscope was used to obtain the fluorescence images.

This article is protected by copyright. All rights reserved

The competition test of target protein

A competition test was established to determine the binding site of SW and AKT. The maleic anhydride 96-well plates were activated by wash buffer according to the instructions. The amino bridging agent solution (10 μg/mL) was dissolved in the immobilization buffer. Then, 100 μL of amino bridging agent solution was added to each well. After incubating on a shaker for 3 h at room temperature, the amino bridging agent solution was removed from the plate wells. 10 μg/mL probe 1 and the catalyst solution were added to each well to click reaction for probe 2 preparation. AKT crude proteins were extracted from liver of mice, purified by ammonium sulfate precipitation, and desalted by ultrafiltration. AKT crude proteins (1 mg/mL) were added to each well. In the same way, 20 μg/mL AKT-PH domain purified proteins were added to the wells, respectively. The plate was incubated on a shaker for 12 h at 4°C to capture target proteins. Then, 100 μL of different AKT inhibitor solutions at 100 μg/mL were added to each well and competed with probe 2 against enriched target proteins for next 12 h at 4°C on a shaker. After washing with PBST, the residual AKT protein was detected by the ELISA process via anti-AKT antibody. The absorbance values of TMB (3, 3′, 5, 5′-Tetramethylbenzidine) substrate were determined by a BioTek Elx800 microplate reader at 450 nm (BioTek Instruments, Inc. USA).

AKT plasma translocation assay

To evaluate the AKT translocation efficiency, HEK 293T cells were transfected with $AKT^{PH(R25)}$-GFP and $AKT^{PH(R25C)}$-GFP plasmids to express $AKT^{PH(R25)}$-GFP and $AKT^{PH(R25C)}$-GFP fusion protein. AKT-$PH^{(R25C)}$, which harbored mutated amino acid sites in the PH domain of AKT that prevents the transfer to the membrane, served as a negative control [18]. SC79 served as a positive control as it can reverse the transfer of PH domain. Cells were cultured in small confocal dishes for 24 h. Different concentrations of SC79 and SW were added to the cells before transfection. Then, cells were starved with $AKT^{PH(R25)}$-GFP and $AKT^{PH(R25C)}$-GFP plasmids for 6 h, separately. Cell membrane fluorescent dye Dil (5 μM) was added to the cells for 10 min for membrane location. To detect the effect on AKT translocation, fluorescent photos of the cells were taken immediately after plasmid translocation. The excitation and emission wavelengths of GFP were 488 nm and 507 nm, and for Dil were 549 nm and 565 nm, respectively.

This article is protected by copyright. All rights reserved

Accepted Article

Western blot and inflammatory cytokines assay

HEK 293T cells were cultured in 6-wells plates for 12 h. Then PHT-427 (10 μM) and different concentration of SW (0.1-10 μM) were added to the cells for 6 h. Cell Lysates were collected after that for western blot to determine the effect of SW on the basic level of P-AKT. In addition, HEK 293T cells were also used to determine the inhibition effect of SW (0.1-10 μM) on P-AKT after activated by SC79 (10 μM).

BEAS-2B cells were cultured in 6-wells plates for 12 h. Then SW in several concentrations (0.1-10 μM), PHT-427 (10 μM) or Dex (10 μM) were added to cells for preincubation 6 h. TNF-α (10 ng/mL) or LPS (10 μg/mL) were added to cell medium respectively for 15-30 min to induce the activation of AKT. Cell Lysates were collected after that for western blot to determine the effect of SW on AKT phosphorylation. In addition, LPS-induced the expression of cytokines, IL-6, IL-8 and TNF-α were measured with ELISA kits (Wes Tang Bio-Tech, Shanghai, China).

RAW264.7 cells were cultured in 6-wells plates for 12 h. Then SW in several concentrations (0.1-10 μM), PHT-427 (10 μM) were added to cells for 6 h. LPS (10 μg/mL) was added to the cell medium for 15-30 min to induce the activation of AKT. Cell Lysates were also collected for western blot to determine the effect of SW on AKT expression.

Acute lung injury model

Male KM mice (18-22 g) were purchased from SPF Biotechnology Co., Ltd. (Beijing, China). All animal care and experimental protocols were approved by the Instructional Animal Care and Use Committee (IACUC) (TCM-LAEC2016031) and raised under standard specific pathogen-free conditions with 12/12-h light/dark cycles at 23 ± 2°C and free access to water and food.

The mice were divided into six group randomly (eight mice per group): Con, Model (Mod, PA 14), Dex (PA 14 + 5 mg/kg/d Dex), SW-H (PA 14 + 100 mg/kg/d SW), SW-M (PA 14 + 50 mg/kg/d SW), and SW-L (PA 14 + 25 mg/kg/d SW). Mice were administered drugs or physiological saline by intragastric gavage daily for one week. On the eight days, animals were anesthetized by intraperitoneal injection with 10% chloral solution (4 μL/g). Then, an acute lung injury model was induced by dropping activated PA 14 bacterium (1×10^7 /20 μL in PBS) into their nasal cavity. After 24 h, the perfusates (right lung) of mice were collected for further cytokine IL-6, IL-8 and TNF-α assays. The right lung tissues were eviscerated after

This article is protected by copyright. All rights reserved

perfusion for protein-based assays. Left lung tissues of mice were eviscerated and fixed in formaldehyde solution (10%) for hematoxylin-eosin (H&E) staining.

Statistical analysis

All the results were performed as the mean ± standard deviation. The statistical comparison between two groups were performed by t-tests, and for multiple groups by analysis of variance (One-way ANOVA) followed by Bonferroni's test with a single pooled variance test, and $p < 0.05$ was considered to be statistically significant.

Accepted Article

This article is protected by copyright. All rights reserved

Accepted Article

References

1. Cai D & Liu T (2011) Hypothalamic inflammation: a double-edged sword to nutritional diseases, *Ann N Y Acad Sci* **1243**, E1-39.

2. Tracey KJ (2002) The inflammatory reflex, *Nature* **420**, 853-9.

3. Nathan C (2002) Points of control in inflammation, *Nature* **420**, 846-52.

4. Camps J & Garcia-Heredia A (2014) Introduction: oxidation and inflammation, a molecular link between non-communicable diseases, *Adv Exp Med Biol* **824**, 1-4.

5. Fu YW, Zhang QZ, Xu DH, Liang JH & Wang B (2014) Antiparasitic effect of cynatratoside-C from Cynanchum atratum against Ichthyophthirius multifiliis on grass carp, *J Agric Food Chem* **62**, 7183-9.

6. Fu Y, Gao R, Cao Y, Guo M, Wei Z, Zhou E, Li Y, Yao M, Yang Z & Zhang N (2014) Curcumin attenuates inflammatory responses by suppressing TLR4-mediated NF-kappaB signaling pathway in lipopolysaccharide-induced mastitis in mice, *Int Immunopharmacol* **20**, 54-8.

7. Fu Y, Zhou E, Wei Z, Liang D, Wang W, Wang T, Guo M, Zhang N & Yang Z (2014) Glycyrrhizin inhibits the inflammatory response in mouse mammary epithelial cells and a mouse mastitis model, *FEBS J* **281**, 2543-57.

8. De UK & Mukherjee R (2009) Expression of cytokines and respiratory burst activity of milk cells in response to Azadirachta indica during bovine mastitis, *Trop Anim Health Prod* **41**, 189-97.

9. Hou Y, Nie Y, Cheng B, Tao J, Ma X, Jiang M, Gao J & Bai G (2016) Qingfei Xiaoyan Wan, a traditional Chinese medicine formula, ameliorates Pseudomonas aeruginosa-induced acute lung inflammation by regulation of PI3K/AKT and Ras/MAPK pathways, *Acta Pharm Sin B* **6**, 212-21.

10. Hisanaga A, Mukai R, Sakao K, Terao J & Hou DX (2016) Anti-inflammatory effects and molecular mechanisms of 8-prenyl quercetin, *Mol Nutr Food Res* **60**, 1020-32.

11. Ma X, Zhang Y, Wang Z, Shen Y, Zhang M, Nie Q, Hou Y & Bai G (2017) Ursolic Acid, a Natural Nutraceutical Agent, Targets Caspase3 and Alleviates Inflammation-Associated Downstream Signal Transduction, *Mol Nutr Food Res.* **61**.

12. Sandigawad AM (2015) Analysis of phytochemicals and antibacterial potential of Lonicera japonica thunb, *International Journal of Pharma & Bio Sciences* **6**, B571-B583.

This article is protected by copyright. All rights reserved

13. Chen CY, Peng WH, Wu LC, Wu CC & Hsu SL (2010) Luteolin Ameliorates Experimental Lung Fibrosis Both in Vivo and in Vitro: Implications for Therapy of Lung Fibrosis, *Journal of Agricultural & Food Chemistry* **58**, 11653-11661.

14. Bai F, Xu H, Zhang Q, Qi X, Mou R, Bai G & Qiao M (2011) Functional characterization of pfm in protein secretion and lung infection of Pseudomonas aeruginosa, *Canadian Journal of Microbiology* **57**, 829-37.

15. Shang X, Pan H, Li M, Miao X & Ding H (2011) Lonicera japonica Thunb.: ethnopharmacology, phytochemistry and pharmacology of an important traditional Chinese medicine, *Journal of Ethnopharmacology* **138**, 1-21.

16. Jiang M, Han YQ, Zhou MG, Zhao HZ, Xiao X, Hou YY, Gao J, Bai G & Luo GA (2014) The Screening Research of Anti-Inflammatory Bioactive Markers from Different Flowering Phases of Flos Lonicerae Japonicae, *Plos One* **9**, e96214.

17. Chang J, Zhao XM, Liu CX & Zhang TZ (2008) Structure elucidation of metabolites of swertiamarin produced by Aspergillus niger, *J Mol Struct* **878**, 22-25.

18. Zhou M, Ma X, Ding G, Wang Z, Liu D, Tong Y, Zhou H, Gao J, Hou Y, Jiang M & Bai G (2017) Comparison and evaluation of antimuscarinic and anti-inflammatory effects of five Bulbus fritillariae species based on UPLC-Q/TOF integrated dual-luciferase reporter assay, PCA and ANN analysis, *J Chromatogr B Analyt Technol Biomed Life Sci* **1041-1042**, 60-69.

19. Kumar CC & Madison V (2005) AKT crystal structure and AKT-specific inhibitors, *Oncogene* **24**, 7493-501.

20. Calleja V, Laguerre M, Parker PJ & Larijani B (2009) Role of a novel PH-kinase domain interface in PKB/Akt regulation: structural mechanism for allosteric inhibition, *PLoS Biol* **7**, e17.

21. Grimshaw KM, Hunter LJ, Yap TA, Heaton SP, Walton MI, Woodhead SJ, Fazal L, Reule M, Davies TG, Seavers LC, Lock V, Lyons JF, Thompson NT, Workman P & Garrett MD (2010) AT7867 is a potent and oral inhibitor of AKT and p70 S6 kinase that induces pharmacodynamic changes and inhibits human tumor xenograft growth, *Mol Cancer Ther* **9**, 1100-10.

22. Moses SA, Ali MA, Zuohe S, Du-Cuny L, Zhou LL, Lemos R, Ihle N, Skillman AG, Zhang S, Mash

This article is protected by copyright. All rights reserved

EA, Powis G & Meuillet EJ (2009) In vitro and in vivo activity of novel small-molecule inhibitors targeting the pleckstrin homology domain of protein kinase B/AKT, *Cancer Res* **69**, 5073-81.

23. Meuillet EJ (2011) Novel inhibitors of AKT: assessment of a different approach targeting the pleckstrin homology domain, *Curr Med Chem* **18**, 2727-42.

24. Hu TY, Ju JM, Mo LH, Ma L, Hu WH, You RR, Chen XQ, Chen YY, Liu ZQ, Qiu SQ, Fan JT & Cheng BH (2018) Anti-inflammation action of xanthones from Swertia chirayita by regulating COX-2/NF-kappaB/MAPKs/Akt signaling pathways in RAW 264.7 macrophage cells, *Phytomedicine* **55**, 214-221.

25. Chen HW, Lin AH, Chu HC, Li CC, Tsai CW, Chao CY, Wang CJ, Lii CK & Liu KL (2011) Inhibition of TNF-alpha-Induced Inflammation by andrographolide via down-regulation of the PI3K/Akt signaling pathway, *J Nat Prod* **74**, 2408-13.

26. Li M, Shang X, Zhang R, Jia Z, Fan P, Ying Q & Wei L (2010) Antinociceptive and anti-inflammatory activities of iridoid glycosides extract of Lamiophlomis rotata (Benth.) Kudo, *Fitoterapia* **81**, 167-72.

27. Liu X & Wang J (2011) Anti-inflammatory effects of iridoid glycosides fraction of Folium syringae leaves on TNBS-induced colitis in rats, *J Ethnopharmacol* **133**, 780-7.

28. Lu CM, Lin LC & Tsai TH (2014) Determination and pharmacokinetic study of gentiopicroside, geniposide, baicalin, and swertiamarin in Chinese herbal formulae after oral administration in rats by LC-MS/MS, *Molecules* **19**, 21560-78.

29. Magora HB, Rahman MM, Gray AI & Cole MD (2003) Swertiamarin from Enicostemma axillare subsp axillare (Gentianaceae), *Biochem Syst Ecol* **31**, 553-555.

30. Saravanan S, Pandikumar P, Prakash Babu N, Hairul Islam VI, Thirugnanasambantham K, Gabriel Paulraj M, Balakrishna K & Ignacimuthu S (2014) In vivo and in vitro immunomodulatory potential of swertiamarin isolated from Enicostema axillare (Lam.) A. Raynal that acts as an anti-inflammatory agent, *Inflammation* **37**, 1374-88.

31. Saravanan S, Islam VI, Thirugnanasambantham K, Pazhanivel N, Raghuraman N, Paulraj MG & Ignacimuthu S (2014) Swertiamarin ameliorates inflammation and osteoclastogenesis intermediates in IL-1beta induced rat fibroblast-like synoviocytes, *Inflamm Res.* **63**, 451-62.

This article is protected by copyright. All rights reserved

32. Saravanan S, Islam VI, Babu NP, Pandikumar P, Thirugnanasambantham K, Chellappandian M, Raj CS, Paulraj MG & Ignacimuthu S (2014) Swertiamarin attenuates inflammation mediators via modulating NF-kappaB/I kappaB and JAK2/STAT3 transcription factors in adjuvant induced arthritis, *Eur J Pharm Sci* **56**, 70-86.

33. Dinarello CA (2010) Anti-inflammatory Agents: Present and Future, *Cell* **140**, 935-50.

34. Manning BD & Toker A (2017) AKT/PKB Signaling: Navigating the Network, *Cell* **169**, 381-405.

35. Jo H, Mondal S, Tan D, Nagata E, Takizawa S, Sharma AK, Hou Q, Shanmugasundaram K, Prasad A, Tung JK, Tejeda AO, Man H, Rigby AC & Luo HR (2012) Small molecule-induced cytosolic activation of protein kinase Akt rescues ischemia-elicited neuronal death, *Proc Natl Acad Sci U S A* **109**, 10581-6.

36. Calleja V, Laguerre M & Larijani B (2009) 3-D structure and dynamics of protein kinase B-new mechanism for the allosteric regulation of an AGC kinase, *J Chem Biol.* **2**, 11-25.

37. Blagg J & Workman P (2017) Choose and Use Your Chemical Probe Wisely to Explore Cancer Biology, *Cancer Cell* **32**, 268-270.

38. Andjelkovic M, Alessi DR, Meier R, Fernandez A, Lamb NJ, Frech M, Cron P, Cohen P, Lucocq JM & Hemmings BA (1997) Role of translocation in the activation and function of protein kinase B, *J Biol Chem* **272**, 31515-24.

39. Lucic I, Rathinaswamy MK, Truebestein L, Hamelin DJ, Burke JE & Leonard TA (2018) Conformational sampling of membranes by Akt controls its activation and inactivation, *Proc Natl Acad Sci U S A* **115**, E3940-E3949.

40. Berndt N, Yang H, Trinczek B, Betzi S, Zhang Z, Wu B, Lawrence NJ, Pellecchia M, Schonbrunn E, Cheng JQ & Sebti SM (2010) The Akt activation inhibitor TCN-P inhibits Akt phosphorylation by binding to the PH domain of Akt and blocking its recruitment to the plasma membrane, *Cell Death Differ* **17**, 1795-804.

41. Han DD, Chen W, Gu XL, Shan RX, Zou JQ, Liu G, Shahid M, Gao J & Han B (2017) Cytoprotective effect of chlorogenic acid against hydrogen peroxide-induced oxidative stress in MC3T3-E1 cells through PI3K/Akt-mediated Nrf2/HO-1 signaling pathway, *Oncotarget* **8**, 14680-14692.

42. Weyrich P, Neuscheler D, Melzer M, Hennige AM, Haring HU & Lammers R (2007) The

This article is protected by copyright. All rights reserved

Accepted Article

Par6alpha/aPKC complex regulates Akt1 activity by phosphorylating Thr34 in the PH-domain, *Mol Cell Endocrinol* **268**, 30-6.

43. Thomas CC, Deak M, Alessi DR & van Aalten DM (2002) High-resolution structure of the pleckstrin homology domain of protein kinase b/akt bound to phosphatidylinositol (3,4,5)-trisphosphate, *Curr Biol* **12**, 1256-62.

Supporting information

Figure S1. Synthetic route for compound 3 (probe 1).

Figure S2. The NMR data of compound 3.

Figure S3. Synthetic route for compound 7 (an amino bridging agent).

Figure S4. The NMR data of compound 5.

Figure S5. The NMR data of compound 6.

Figure S6. The NMR data of compound 7.

Figure S7. The Purification of AKT-PH domain.

Figure S8. SW no longer act anti-inflammatory on an AKT-null background.

Figure S9: SW induced cell apoptosis.

Figure S10: The impact of SW in HEK 293T cell cycle.

This article is protected by copyright. All rights reserved

Accepted Article

Figure Legends

Figure 1. The synthesis and application process of SW probe 1 for target fishing. (A) Synthesis of azide-swertiamarin (probe 1) and the application of probe 1 in target fishing. (B) The effects of SW and probe 1 on TNF-α-induced NF-κB expression (n = 6). (C) Fishing and identifying potential protein targets. SDS-PAGE (left panel) and western blot analysis (right panel) were used to detect the captured proteins. Lane 1 was total protein from BEAS-2B cell lysate; lanes 2 and 3 were proteins enriched from BEAS-2B cells by absMMs and probe 1-modified absMMs. (D) The interaction analyzing of potential anti-inflammatory targets of SW, which predicted by String 10.1. Bars represent mean ± SD, $^{*}p < 0.05$, $^{**}p < 0.01$, $^{***}p < 0.001$ compared with the model group. $^{###}p< 0.001$ compared with the Con group, by One-way ANOVA with Bonferroni post-test.

Figure 2. Synthesis of the fluorescent probe SW-CY5 and application of co-localization. (A) Synthesis of the fluorescent click product with probe 1 and alkynyl CY5. (B) Co-localization of AKT antibody (green) and SW (red) in BEAS-2B cells.

Figure 3. SW targets AKT-PH domain. (A) The synthesis scheme of an amino bridging agent; the process of preparation of solidified-probe 2 and the capture of AKT proteins. (B) The effect of AKT crude proteins extracted from mouse liver (left panel) or purified AKT-PH domain proteins (right panel) captured by probe 2 and competed with different inhibitors. Con group was alkynyl maleic anhydride activated plate (n = 3). Bars represent mean ± SD, $^{***}p < 0.001$ compared with the model group. $^{###}p < 0.001$ compared with the Con group, by One-way ANOVA with Bonferroni post-test.

This article is protected by copyright. All rights reserved

Figure 4. SW led to dissociation of membrane-bound AKT-PH domain. (A) SW-affected membrane translocation of AKT-PH in a dose-response manner (0.1-10 μM). Representative images showed the membrane translocation of the AKT-PH domain with SC79 (10 μM) or SW (0.1-10 μM) treatment. $AKT^{PH(R25)}$-GFP and $AKT^{PH(R25C)}$-GFP were used as the positive and negative control, respectively. The histogram presented the fluorescence ratios of $AKT^{PH(R25)}$-GFP/Dil on HEK 293T membranes (n = 6). (B) Schematic model of SW-induced AKT deactivation. Bars represent mean ± SD, $^{***}p<0.01$ compared with the R25 group, by One-way ANOVA with Bonferroni post-test.

Figure 5. SW inhibited AKT activity and down-regulated the phosphorylation of AKT by acting on the PH domain of AKT. (A) SW inhibited the activation of AKT in HEK 293T cells induced by SC79. (B) SW reduced the basal level of P-AKT in HEK 293T cells (n = 3). (C) SW decreased the level of P-AKT activated by AKT activator SC79 in HEK 293T cells (n = 3). (D) Molecular docking of SW, PHT-427 and SC79 with the AKT PH domain (PDB:1UNQ). Here, PyMOL software was used to display the 3D maps of the protein-ligand interaction, and MOE software was used to display the 2D depiction of the protein-ligand interaction. Bars represent mean ± SD, by One-way ANOVA with Bonferroni post-test. ##p< 0.01 compared with the Con group, *p < 0.05, **p < 0.01 compared with the SC79 group: A; **P < 0.01, ***P < 0.001 compared with the Con group: B; ***P < 0.001 compared with the model group; ###P < 0.001 compared with the Con group: C.

Figure 6. SW deactivated the phosphorylation of AKT on both Ser473 and Thr308 and inhibited the downstream inflammatory molecules of AKT. (A) SW attenuated 10 μg/mL LPS-induced phosphorylation of AKT on both Ser473 and Thr308 in RAW264.7 cells (n = 3). (B) SW attenuated TNF-α (10 ng/mL) induced phosphorylation of AKT on both Ser473 and Thr308 in BEAS-2B cells. PHT-427 worked as a positive control (n = 3). (C) SW attenuated LPS (10 μg/mL) induced phosphorylation of AKT, IKK and NF-κB in BEAS-2B cells (n = 3). (D) SW inhibited the production of TNF-α, IL-6 and IL-8 induced by LPS. Each bar represents mean ± SD (n = 6). Bars represent mean ± SD, $^{*}P < 0.05$, $^{**}P < 0.01$, $^{***}P < 0.001$ compared with the model group; $^{\#}P < 0.05$, $^{\#\#}P < 0.01$, $^{\#\#\#}P < 0.001$ compared with the Con group, by One-way ANOVA with Bonferroni post-test.

This article is protected by copyright. All rights reserved

Figure 7. The effect of SW on PA 14-induced acute lung injury. (A) SW attenuated PA 14-induced phosphorylation of AKT, IKK, and NF-κB (n = 3). (B) H&E staining images of the lungs (left side, 10×; right side, 400×). SW inhibited the production of TNF-α (C), IL-6 (D) and IL-8 (E) induced by PA 14 (n = 8). Bars represent mean ± SD, $^{*}p < 0.05$, $^{**}p < 0.01$, $^{***}p < 0.001$ compared with the model group; $^{\#\#}p< 0.01$, $^{\#\#\#}p< 0.001$ compared with the Con group, by One-way ANOVA with Bonferroni post-test.

Acknowledgements

This study was supported by National Natural Science Foundation of China (Numbers 81673616), International Cooperation and Exchange of the National Natural Science Foundation of China (Numbers 81761168039), and the Fundamental Research Funds for the Central Universities, Nankai University (Grant Number 63191723)

Authors contributions

G. B. and Y. H. designed the study; M.Z. performed experiments, acquired and analyzed data, drafted and edited the manuscript; X.M. performed Co-localization; H.X. synthesized SW probe 1; H.X. expressed and purified AKT-PH domain proteins; W.W. assisted with animal experiments; X.W. and M.J. assisted with experiments. G. B., Y. H., and M.Z. contributed to data discussion and review of the manuscript.

Conflict of Interest

The authors declare no conflict of interest.

This article is protected by copyright. All rights reserved

Accepted Article

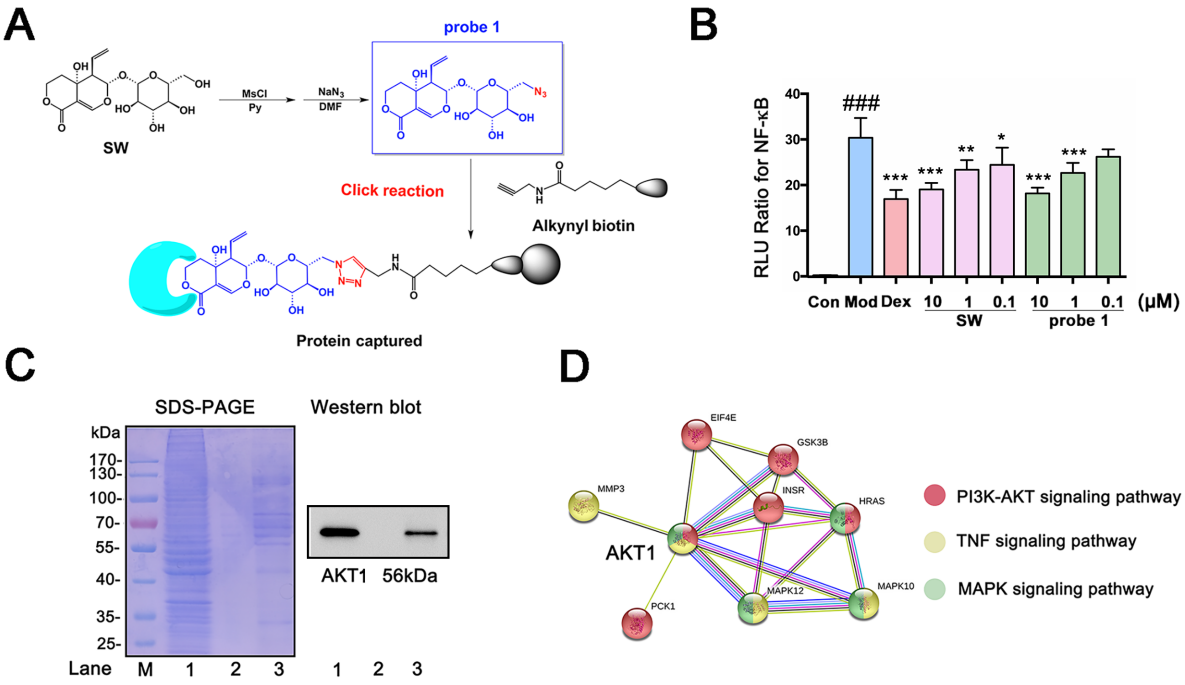

febs_15112_f1.tif

This article is protected by copyright. All rights reserved

Accepted Article

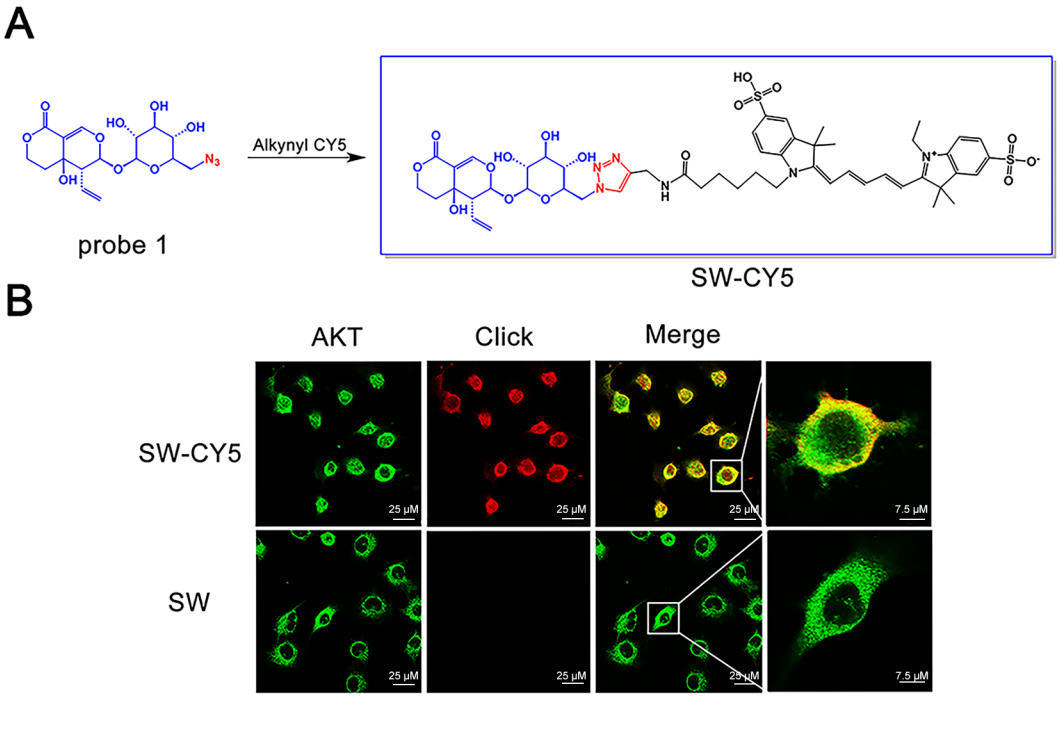

febs_15112_f2.tif

This article is protected by copyright. All rights reserved

Accepted Article

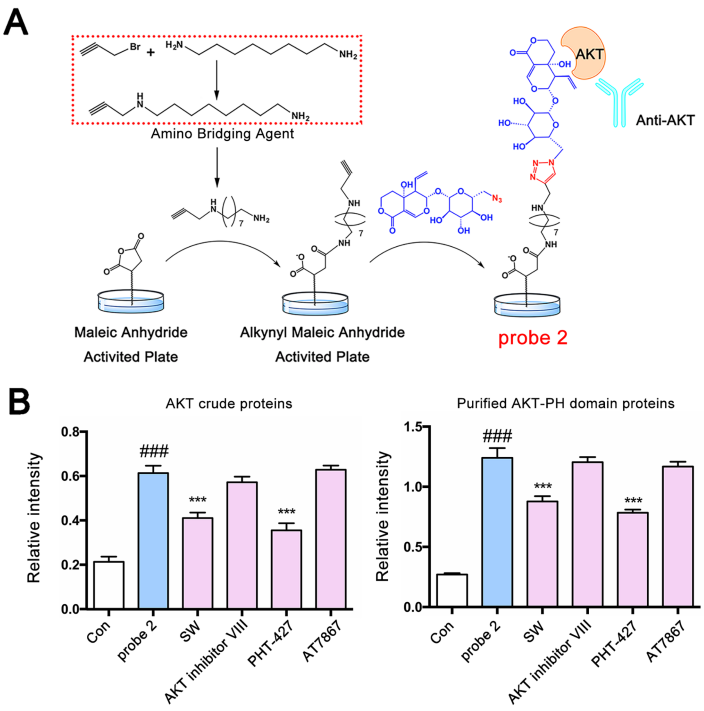

febs_15112_f3.tif

This article is protected by copyright. All rights reserved

Accepted Article

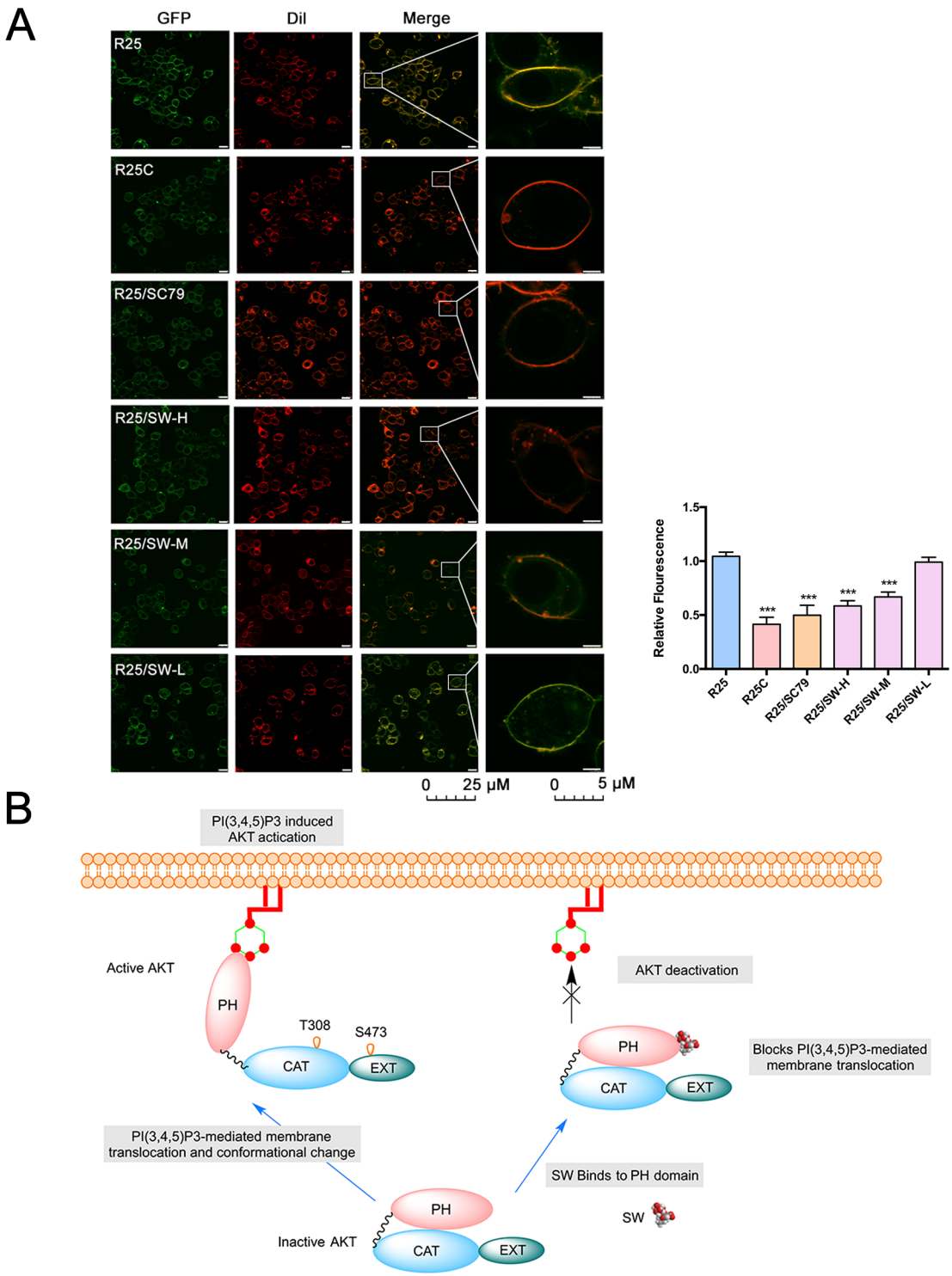

febs_15112_f4.tif

This article is protected by copyright. All rights reserved

Accepted Article

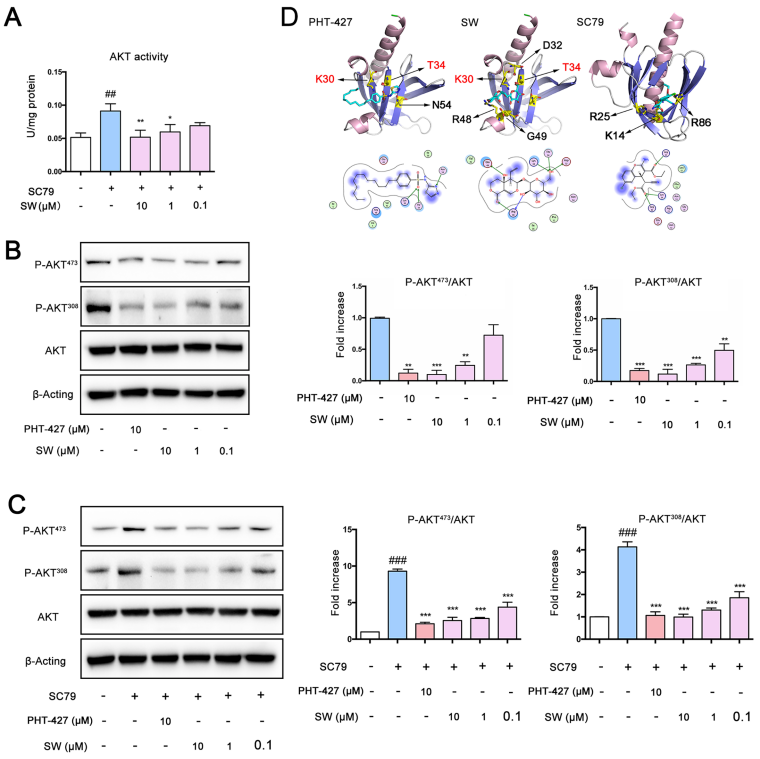

febs_15112_f5.tif

This article is protected by copyright. All rights reserved

Accepted Article

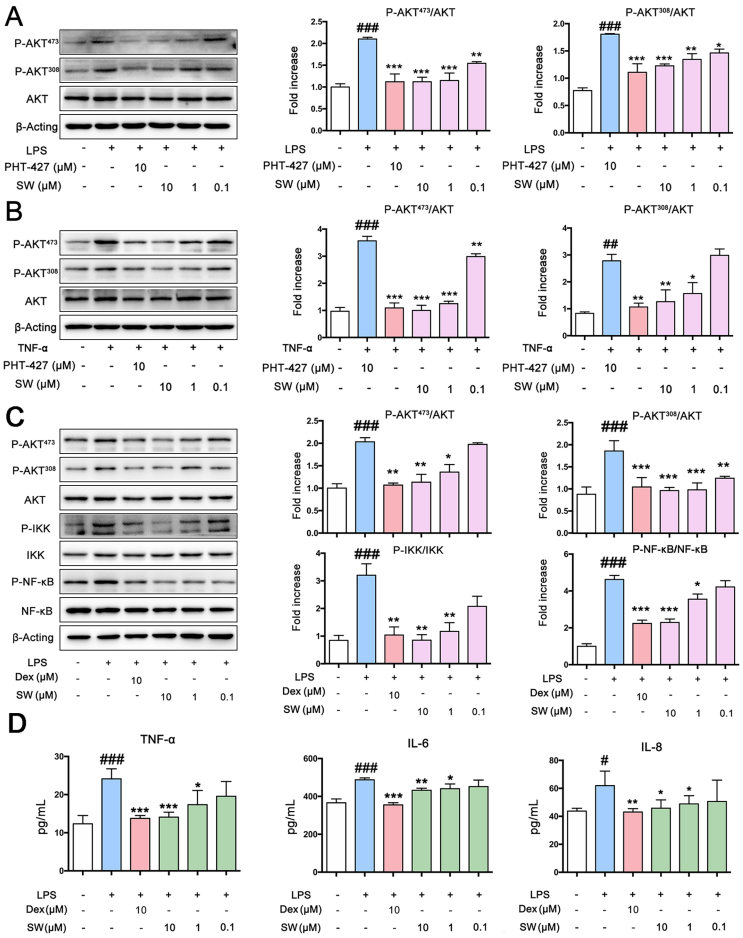

febs_15112_f6.tif

This article is protected by copyright. All rights reserved

Accepted Article

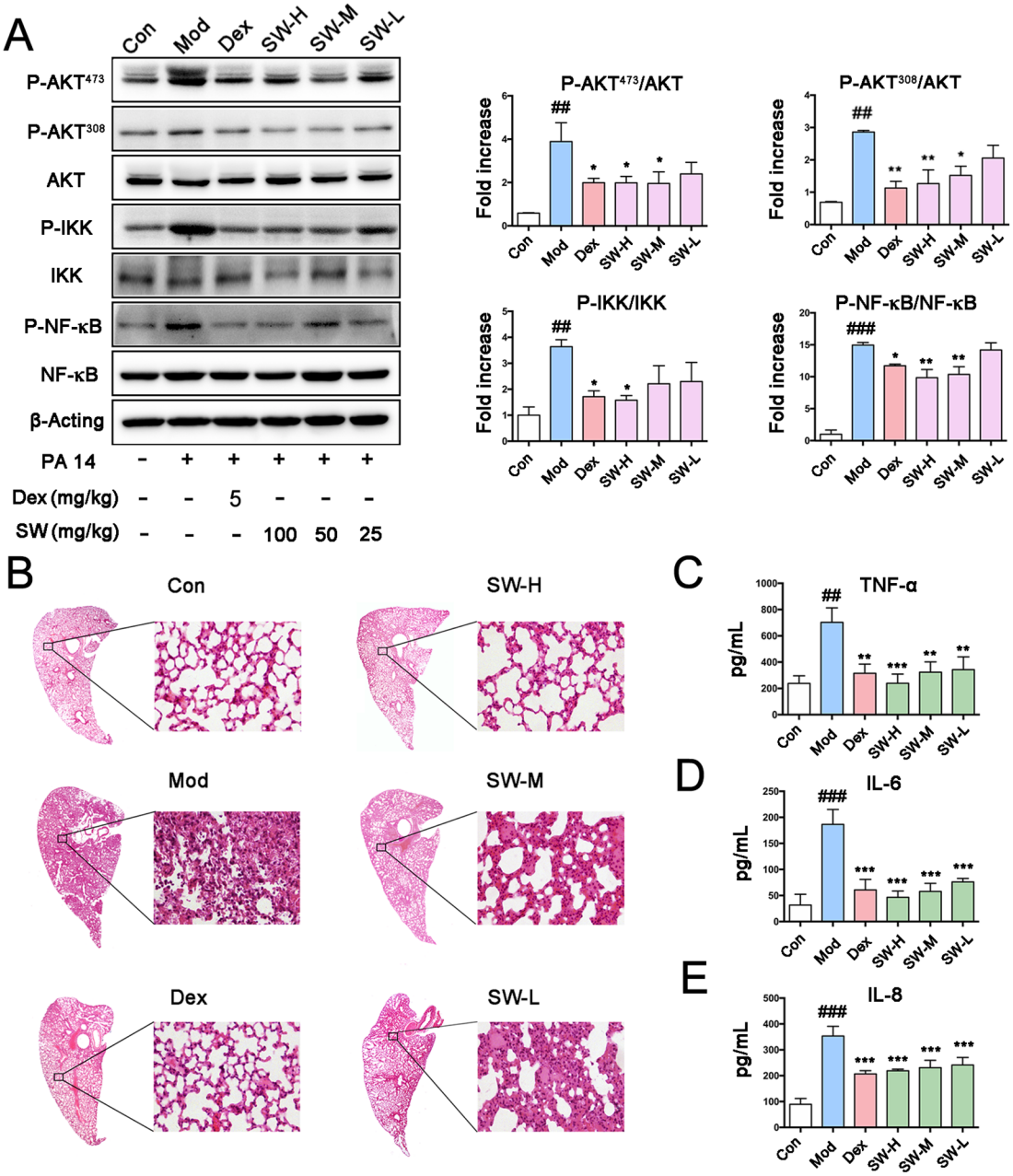

febs_15112_f7.tif

This article is protected by copyright. All rights reserved